



# Freeze-thaw processes of active layer regulate soil respiration of alpine meadow in the permafrost region of the Qinghai-Tibet Plateau

5 Junfeng Wang<sup>1,2</sup>, Qingbai Wu<sup>1</sup>, Ziqiang Yuan<sup>1</sup>, Hojeong Kang<sup>3</sup>

<sup>1</sup> State Key Laboratory of Frozen Soil Engineering, Northwest Institute of Eco-Environment and Resources, CAS, Lanzhou 730000, China

<sup>2</sup> Beiluhe Observation Station of Frozen Soil Environment and Engineering, Northwest Institute of  
10 Eco-environment and Resources, CAS, Lanzhou 730000, China

<sup>3</sup> School of Civil and Environmental Engineering, Yonsei University, Seoul 03722, Korea

*Correspondence to:* Hojeong Kang (hj\_kang@yonsei.ac.kr)

**Abstract:** Freezing and thawing action of the active layer plays a significant role in soil respiration ( $R_s$ ) in permafrost regions. However, little is known about how the freeze-thaw process regulates  
15 the  $R_s$  dynamics in different stages for the alpine meadow underlain by permafrost on the Qinghai-Tibet Plateau (QTP). We conducted continuous in-situ measurements of  $R_s$  and freeze-thaw process of the active layer at an alpine meadow site in the Beiluhe permafrost region of QTP to determine the regulatory mechanisms of the different freeze-thaw stages of the active layer on the  $R_s$ . We found that the freezing and thawing process of active layer modified the  $R_s$  dynamics differently in  
20 different freeze-thaw stages. The mean  $R_s$  ranged from 0.56 to 1.75  $\mu\text{mol}/\text{m}^2\text{s}$  across the stages, with the lowest value in the SW stage and highest value in the ST stage; and  $Q_{10}$  among the different freeze-thaw stages changed greatly, with maximum (4.9) in the WC stage and minimum (1.7) in the SW stage. Patterns of  $R_s$  among the ST, AF, WC, and SW stages differed, and the corresponding contribution percentages of cumulative  $R_s$  to annual total  $R_s$  were 61.54, 8.89, 18.35, and 11.2%,  
25 respectively. Soil temperature ( $T_s$ ) was the most important driver of  $R_s$  regardless of soil water status in all stages. Our results suggest that as the climate warming and permafrost degradation continue, great changes in freeze-thaw process patterns may trigger more  $R_s$  emissions from this ecosystem because of prolonged ST stage.

**Keywords:** Soil respiration; Different freeze-thaw stage;  $Q_{10}$ ; Alpine meadow; Qinghai-Tibet  
30 Plateau

## 1 Introduction

Soil respiration ( $R_s$ ) is a significant source in estimating terrestrial carbon budget under climate change. It is the second-largest source of carbon emissions between the atmosphere and the  
35 terrestrial ecosystem on a global scale (Bond-Lamberty and Thomson, 2010; Schlesinger and Andrews, 2000). In permafrost regions,  $R_s$  not only depends on the distribution of vegetation and the content of soil organic matter (SOM) (Ping et al., 2008; Grogan and Chapin Iii, 2000; Phillips et al., 2011; Jobbágy and Jackson, 2000), but also is regulated by the freeze-thaw process of active layer (Holleisen et al., 2011). What's more, many studies have shown that the winter-time emissions



40 contribute significantly to the annual CO<sub>2</sub> balances. For example, the Arctic tundra ecosystem is  
becoming a consistent source of CO<sub>2</sub> because of the CO<sub>2</sub> emission in winter offsetting the CO<sub>2</sub>  
uptake in growing season with progressive permafrost thaw and active layer thickening (Celis et al.,  
2017). In Alaska, emissions of CO<sub>2</sub> from tundra during early winter seasons increased by about 73%  
since 1975, and the Arctic ecosystems has been a net source of CO<sub>2</sub> due to rising temperatures  
45 (Commane et al., 2017). For the sub-arctic tundra ecosystem, the winter-time CO<sub>2</sub> loss also increases  
due to sustained tundra warming and the ecosystem historical function is shifting away from a  
carbon sink to a carbon source (Lüers et al., 2014; Webb et al., 2016). In permafrost regions on  
northern hemisphere, the amount of soil organic carbon (SOC) stored reaches 1832Pg (Ding et al.,  
2015; Mu et al., 2015), among which 495.8Pg distributes in the 0-1m depth, 1024Pg in the 0-3m  
50 depth and 648 Pg in the 3-25m depth (Mu et al., 2015). Due to its high sensibility to global warming  
and direct contribution to the atmosphere greenhouse gas contents, the carbon emission from  
permafrost has received worldwide attention (Tarnocai, 2009; Zimov et al., 2009).

In the scenario of global warming, the active layer and permafrost distributed in the Arctic and  
mid-latitude alpine regions are undergoing significant changes (Jorgenson and Osterkamp, 2005).  
55 The active layer, acting as a buffer between permafrost and atmosphere, is more sensitive and  
responds more quickly to climate change (Li et al., 2012). The energy and water exchange in  
permafrost regions between the earth and atmosphere is mainly completed by the active layer.  
However, in a whole freeze-thaw cycle, the active layer will undergo a series of processes of cooling,  
start freezing to fully freezing, dropping in temperature, rising in temperature but still in frozen state,  
60 start thawing to fully thawing, and rising in temperature but in thawed state (Jiao and Li, 2014). At  
different developing stages of freeze-thaw cycling, the heat distribution and transmission in the  
active layer show significantly different characteristics (Zhao et al., 2000). Thus the soil  
physicochemical properties, microbial activities, and biogeochemical processes at different freeze-  
thaw stages are also different from each other (Henry, 2007). So the dynamics of  $R_s$  emission at  
65 different freeze-thaw stages will show apparent differences. Furthermore, the thawing of the  
permafrost and the deepening of the active layer will expose the frozen organic carbon to microbial  
decomposition and cause previously frozen SOC to become available for mineralization (Walz et  
al., 2017), and thus may accelerate a positive permafrost carbon feedback on climate (Schuur et al.,  
2008). A study of six years of CO<sub>2</sub> flux measurements in a moist acidic tundra has shown that the  
70 active layer thickness is a key driver of NEE, GPP, and ecosystem respiration (Celis et al., 2017). In  
the high-altitude mountain regions, thawing permafrost has caused the alpine tundra to release long-  
frozen CO<sub>2</sub> to the atmosphere, exacerbating climate warming (Knowles et al., 2019). Therefore,  
permafrost will play a significant role in the carbon-climate feedbacks due to its intensity of climate  
forcing and the size of the carbon pools in permafrost regions (MacDougall et al., 2012; Schneider  
75 von Deimling et al., 2012).

The strength and timing of permafrost carbon feedback greatly depend on the freeze-thaw  
process of the active layer and the distribution of SOC in the permafrost regions. Therefore,  
understanding the effects of freeze-thaw actions on the  $R_s$  at different freeze-thaw stages is critical  
for better predicting future climate changes. However, how the freeze-thaw actions at different  
80 stages regulate the  $R_s$  is still unclear and incomprehensive.

The Qinghai-Tibet Plateau (QTP) of China has the largest extent of permafrost in the low-  
middle latitudes of the world and is very sensitive to global climate change (Liu and Chen, 2000; Wu  
et al., 2010). The soil organic carbon (SOC) pools in the permafrost regions on the QTP were



85 estimated to be  $160 \pm 87$  Pg, which was approximately 8.7% of those in the northern circumpolar  
permafrost region (Mu et al., 2015). However, the freeze-thaw occurrence, active-layer thickness,  
and near-surface permafrost temperature have been undergoing dramatic changes in recent years. In  
permafrost regions distributed with alpine meadow ecosystem on the QTP between 2002 and 2012,  
the average onset of spring thawing at 50-cm depth advanced by at least 16 days; the duration of  
thaw increased by at least 14 days; the active-layer thickness increased by  $\sim 4.26$  cm/a and the near-  
90 surface permafrost temperature at 6m and 10m depths increased by  $\sim 0.13$  °C and  $\sim 0.14$  °C,  
respectively (Wu et al., 2015). Therefore, the  $R_s$  of the alpine meadow must be influenced and  
changed dramatically due to the variations of freeze-thaw occurrence, active-layer thickness, and  
near-surface permafrost temperature.

We took in-situ measurements of  $R_s$  and freeze-thaw process of the active layer in an alpine  
95 meadow from January 2017 to December 2018. The objectives were (1) to determine the dynamics  
of the  $R_s$  during a complete freeze-thaw process of active layer; (2) to compare the  $R_s$  patterns among  
the different freeze-thaw stages and its contribution to annual soil CO<sub>2</sub> emission in this region; and  
(3) to establish a preferable  $R_s$  model to accurately predict the soil CO<sub>2</sub> emission of each freeze-  
thaw stages.

## 100 2 Materials and methods

### 2.1 Study site

The experiment was conducted in an alpine meadow ecosystem of the Beiluhe region ( $34^{\circ} 49'$   
 $25.8''$  N,  $92^{\circ} 55' 45.1''$  E), in the hinterland of the QTP, China. The study site represents an area of  
151.6 km<sup>2</sup>, with an altitude of 4600 – 4800 m, which is underlain by permafrost with an active layer  
105 at 1.1-2.3m. The mean annual temperature is  $-3.60$  °C, which is colder than that of other areas in the  
QTP (Yin et al., 2017). The mean annual precipitation is 423.79 mm, 80% of which falls during the  
growing season (from May to September). The air pressure is approximately 550 hPa. The alpine  
meadow represents the most common vegetation type in this area (70%) (Wang and Wu, 2013; Zhang  
et al., 2015b). The alpine meadow ecosystem mainly consists of cold meso-perennial herbs that  
110 grow in conditions where a moderate amount of water is available. The ecosystem's vegetation  
mainly consists of *Kobresia pygmaea* (C. B. Clarke), *Kobresia humilis* (C. A. Meyer ex Trautvetter)  
*Sergievskaja*, *Kobresia capillifolia* (Decaisne) (C. B. Clarke), *Kobresia myosuroides* (Villars) Fiori,  
*Kobresia graminifolia* (C. B. Clarke), *Carex atrofusca Schkuhr subsp.* (minor) (Boott) T. Koyama),  
and *Carex scabriostriis* (Kukenthal) (Chen et al., 2017).

### 115 2.2 Measurement of the freeze-thaw process of the active layer

In the study site, one flat terrain with vegetation coverage of above 70% was selected to  
establish the active layer observation site. According to the active layer lithology and practical  
conditions, soil temperature and soil moisture probes were installed at different depths. The  
installation depths for the soil temperature probes were 5, 20, 50, 80, 120, 150, 180 and 230cm,  
120 respectively; and the depths for the soil moisture probes were 5, 20, 50, 80, 120, 150 and 180cm,  
respectively. Soil temperature was measured using thermistors made by the State Key Laboratory  
of Frozen Soil Engineering (SKLFSE, China), and their temperature accuracy is  $\pm 0.05$ °C. Soil  
moisture was measured using calibrated soil moisture sensors (EC-5, Decagon USA), and their  
moisture accuracy is  $\pm 2\%$ . The soil moisture measured using the EC-5 probe represents the  
125 volumetric water content of liquid water per total soil volume. These measurements were collected



automatically every 30 min by a data logger (CR3000, Campbell Co., USA).

Utilizing the measurements collected by soil temperature probes and a datalogger, the soil hourly mean temperature ( $T_{ave}$ ), the maximum temperature ( $T_{max}$ ), and the minimum temperature ( $T_{min}$ ) of each day at different depths were calculated. According to the  $T_{ave}$  values and assuming that the soil particle surface energy and the salinity of soil having no influence on the soil freezing temperature (Jiao and Li, 2014), the date on which hourly  $T_{ave}$  continued to be lower or higher than 0 °C was regarded as the onset freezing or onset thawing date, respectively (Yang et al., 2002). While the date on which if  $T_{max}$  was greater than 0 °C but  $T_{min}$  less than 0 °C was regarded as the soil was undergoing the daily freeze-thaw process. That is, the soil absorbs heat and thaws during the daytime while it releases heat and freezes during the nighttime, showing a daily freeze-thaw cycling phenomenon. Thus the whole freeze-thaw process of active layer can be divided into different stages.

For the freezing or thawing thickness of the active layer in the freeze-thaw process, the freeze or thaw depth was estimated by linearly interpolating soil temperature profiles between two neighboring points above and below the 0°C isotherm (Wu et al., 2010). The freezing or thawing thickness of the active layer was estimated from daily soil temperature measurements.

### 2.3 Soil respiration measurement

For measuring the  $R_s$ , six 5 × 5m measurement plots were randomly selected around the active layer observation site, and one polyvinyl chloride (PVC) collar (20 cm in internal diameter and 10 cm in height) was inserted into each plot at a depth of 8 cm into the soil with a chamber offset of 2 cm before the soil froze. All the PVC collars were left in place until the end of the study.  $R_s$  flux was measured using an LI-8100A automated soil gas flux system (LI-COR Inc., Lincoln, NE, USA). Living plants inside the collar were removed carefully at the soil surface at least one day before the measurement.  $R_s$  flux was measured for two years covering a complete freeze-thaw cycle of active layer between 2017 and 2018.

$R_s$  flux was determined once every two or three days during the thawing period and once every seven days during the freezing period due to harsh environmental conditions and lack of manpower. Measurements were made between 9:00 and 11:30 a.m. local time on every sampling day to represent the daily average flux based on the diurnal measurements (Zhang et al., 2015a). At the same time, using the thermocouple probe and the ECH2O soil moisture sensor (LI-COR, Lincoln, NE, USA) connected to the LI-8100A, soil temperature ( $T_s$ ) and soil volumetric water content (SWC) at 5cm depth were determined as the soil CO<sub>2</sub> flux measurement besides the collars.

### 2.4 Temperature sensitivity and scaling for $R_s$ at different freeze-thaw stage

The dependency of measured  $R_s$  flux on temperature was determined by fitting the following equation over soil temperature at 5cm depth for the best regression coefficient (Zhang et al., 2015a),

$$R_s = \beta_0 e^{\beta_1 T} \quad (1)$$

where  $R_s$  is the measured soil respiration rate ( $\mu\text{molm}^{-2}\text{s}^{-1}$ ),  $T$  is soil temperature (°C) at 5cm depth, and  $\beta_0$  and  $\beta_1$  are constants. This exponential relationship is commonly used to represent soil respiration and soil carbon efflux as functions of temperature (Janssens and Pilegaard, 2003; Davidson et al., 1998).  $Q_{10}$  represents the temperature sensitivity of  $R_s$ , which is a measure of change in reaction rate at intervals of 10°C and is based on Van't Hoff's empirical rule (Lloyd and Taylor, 1994).  $Q_{10}$  was calculated as the following equation (Davidson and Janssens, 2006; Davidson et al., 1998).



$$Q_{10} = e^{10\beta_1} \quad (2)$$

170 The daily average  $R_s$  flux at the different freeze-thaw stage was obtained by interpolating the average  $R_s$  flux rate between the sampling dates. The total  $R_s$  emission at the different freeze-thaw stage was calculated by computing the sum of products of the average flux rate and the start-stop-time of the different freeze-thaw stage of the active layer as follows (Zhang et al., 2017),

$$SR = \sum_k^m R_{mk} \times \Delta t \quad (3)$$

175 where  $k$  and  $m$  are the corresponding onset date and end date of each freeze-thaw stage, respectively;  $\Delta t$  is the length of occurrence days of each freeze-thaw stage;  $R_{mk}$  is the daily average  $R_s$  rate over the specific freeze-thaw stage.

## 2.5 Statistical analysis

180 Repeated measures ANOVA was applied for testing the statistical significance of the difference among the freeze-thaw stages. Regression analysis was performed between  $R_s$  and soil temperature and soil moisture. All statistical analyses were performed at a significance level of 0.05 and were completed using SPSS 16.0 (SPSS Inc., Chicago, IL, USA).

## 3 Results

### 3.1 Division of different freeze-thaw stage of the active layer

185 In the condition that the effects of the surface energy of the soil particles and salinity in the soil on the freezing temperature could be neglected, we assumed that the soils began to freeze when the temperature dropped to be less than 0°C and to thaw when the temperature was continuously greater than 0°C. Basing on the two years' continuous observation on the freezing and thawing of the active layer in the study site, it can be found that from late April the contour outline of 0°C began to slowly develop downward from the soil surface and got to the maximum depth in the early October (Figure 1), indicating that the surface soil of the active layer began to thaw in late April and the thawing depth reach the maximum in early October. The maximum thawing depth of the active layer was 1.98m in 2017 and 1.89m in 2018. During this thawing period, the isotherm of 0°C changed gently. However, the isotherm of 0°C changed rapidly from early October to late November, showing that 190 the whole active layer froze from the surface to the bottom in a short period of time. According to the variation in characteristics of soil temperature in the active layer, the freezing and thawing cycle process of the active layer can be divided into four different stages: summer thawing stage (ST), autumn freezing stage (AF), winter cooling stage (WC), and spring warming stage (SW).

200 The process of the ST stage started from the time when the soil of the active layer began to thaw downwards from the surface in late April to that when the thawing depth reached the maximum in early October. In this stage, the temperatures decreased as the soil deepened. The whole active layer was in an endothermic process where the heat transferred downward continuously and the soil thawing front also slowly moved downward. For the AF stage, once the thawing depth reached the maximum, the soil began to freeze upwards from the bottom of the active layer. Thus the AF lasted 205 till the whole active layer was frozen. According to the moving direction of the freezing front, the AF stage again could be divided into two sub-stages, viz. unidirectional freezing process (UF substage) from down to up and “zero-curtain” process (ZC substage). The UF substage started from the moment when the active layer began to freeze upwards from the bottom and ended when the surface soil started to stably freeze. Meanwhile, the ZC substage started from the moment when the 210 surface soil was stably frozen until the end of the whole freezing process. During the AF, the slope



of 0°C isotherm was small. Especially between the depth of 50cm and 160cm, the 0°C isotherm almost paralleled the axis of ordinate. This phenomenon showed that when the AF process started, the onsets of freezing at different depths had no apparent differences and the whole active layer completed the freezing process in a short time. After the completion of the whole freezing process, the WC process of the active layer quickly started and lasted until mid-late January of the next year. During this process, the soil temperatures were relatively lower in the upper active layer but higher in the bottom. The SW stage started in late January as the air-temperature rose, and the temperature gradients in the active layer gradually decreased. During the SW stage, the surface soil usually underwent daily freezing and thawing cycles in late April. After the above four freeze-thaw stages were finished, the active layer completed a complete freeze-thaw cycle.

Based on the observation data obtained from the experimental site in 2017 and 2018, the start-stop-time and the corresponding duration of each stage were calculated (Table 1). It can be seen that the ST stage started from April 29, 2017, and ended on October 2, 2017, lasting about 157 days. Meanwhile, the AF stage was short and only lasted about 28 days, of which the UF substage lasted for 20 days and the ZC substage 8 days. The stages of WC and SW had a similar time of length and they accounted for 92 and 89 days, respectively.

### 3.2 Dynamics of $R_s$ fluxes in different freeze-thaw stages of the active layer

At the Beiluhe experimental site,  $R_s$  flux changed regularly as the freeze-thaw processes of active layer developed, suggesting that the freezing and thawing processes of active layer regulated the  $R_s$  strongly (Figure 2). In the ST stage,  $R_s$  flux showed a rapidly increasing trend as the thawing of active layer intensified. The  $R_s$  flux rate rose from 0.26 to 2.77  $\mu\text{mol}/\text{m}^2\text{s}$  in 2017 and 0.53 to 2.82  $\mu\text{mol}/\text{m}^2\text{s}$  in 2018. After the ST process finished, the active layer went into the AF stage, in which the  $R_s$  flux fluctuated acutely. In the UF substage, the  $R_s$  flux decreased sharply as the active layer began to freeze from the bottom and the surface soil temperature lowered to freezing point. Thereafter, the active layer went into the ZC substage and the  $R_s$  emission rate again began to increase slowly. In the AF stage, the  $R_s$  flux fluctuated between 1.49 and 2.01  $\mu\text{mol}/\text{m}^2\text{s}$ . After the AF process was completed, the active layer went into the WC stage. As the soil temperature of active layer lowered continuously, the  $R_s$  flux also decreased rapidly. When it came to the end of the WC process, the  $R_s$  flux reached the minimum value of about 0.12 in 2017 and 0.13  $\mu\text{mol}/\text{m}^2\text{s}$  in 2018. Then the  $R_s$  flux began to increase gently as the SW process came up. During the SW stage, the  $R_s$  appeared as a small emission peak when the surface of the active layer underwent daily freezing and thawing cycles. After the small emission peak passed, the  $R_s$  flux dropped a little and then started to ascend again quickly once the ST process arrived.

### 3.3 Contribution of $R_s$ in different freeze-thaw stages of the active layer

Based on the equations (1), (2) and (3), we calculated the models of the soil respiration, the temperature sensitivity ( $Q_{10}$ ) and the sum of  $R_s$  ( $SR$ ) in the different four freeze-thaw stages during the experimental period in the years of 2017 and 2018 (Table 2). The  $SR$  emission during the ST stage (1041.85  $\text{gCO}_2/\text{m}^2$ ) was much higher than that during the other three stages (150.54 to 310.69  $\text{gCO}_2/\text{m}^2$ ). The relative contribution of  $SR$  during each freeze-thaw stage to annual total  $R_s$  ranged from 8.89% to 61.54%. The  $SR$  of the AF stage was the lowest (150.54  $\text{gCO}_2/\text{m}^2$ ), among which the UF-substage and ZC-substage accounted for 89.97 and 60.57  $\text{gCO}_2/\text{m}^2$  respectively, and the corresponding annual contribution rates were 5.31% and 3.58% (Figure 3).



### 3.4 Factors affecting $R_s$ fluxes in different freeze-thaw stages

The  $R_s$  was positively related to soil temperatures, following an exponential ( $Q_{10}$ ) relationship with the 5cm soil temperatures regardless of soil water status during the freeze-thaw stages. When calculated on the basis of the dataset of each stage, the  $Q_{10}$  values were 2.22 ( $R^2=0.69$ ), 1.84 ( $R^2=0.55$ ), 2.38 ( $R^2=0.90$ ), 4.90 ( $R^2=0.80$ ), and 1.70 ( $R^2=0.61$ ) for ST, UF and ZC substages of AF, WC and SW, respectively (Table 2). The soil temperature modified the  $R_s$  dynamics differently in the different freeze-thaw stages (Figure 4). In the ST stage, the variations of  $R_s$ ,  $T_s$ , and SWC were basically consistent. The  $R_s$  showed an increasing trend as  $T_s$  and SWC at 5cm rose due to the active layer thawing from the surface and reached the summit ( $2.42\mu\text{mol}/\text{m}^2\text{s}$ ) till August. Then the  $R_s$  decreased with fluctuations as the  $T_s$  and SWC dropped. When it came to the AF stage, the  $T_s$  and SWC dropped sharply in response to soil freezing, and the  $R_s$  continued to decrease slowly and reached its lowest level ( $1.14\mu\text{mol}/\text{m}^2\text{s}$ ) in mid-October during the UF substage. However, the  $R_s$  increased rapidly to a maximum ( $2.09\mu\text{mol}/\text{m}^2\text{s}$ ) and then dropped quickly with fluctuations although the  $T_s$  and SWC continued to lower during the ZC substage. In the WC stage, the  $R_s$  decreased as the  $T_s$  and SWC lowered continuously, although the active layer was completely frozen. In the SW stage, the  $R_s$  went up again as the  $T_s$  rose in response to soil warming although the SWC had no change because the surface soil still remained frozen in the earlier stage and fluctuated wildly due to daily freeze-thaw process in the later stage.

## 4 Discussion

### 4.1 Magnitude of $R_s$ in the different freeze-thaw stage of the active layer and its

#### $Q_{10}$

Although many studies have showed that freeze-thaw events affect soil respiration ( $R_s$ ) in tundra, boreal, and temperate soils (Liu et al., 2016; Du et al., 2013), the  $R_s$  and  $Q_{10}$  values in different freeze-thaw stages of the active layer are still rarely reported in permafrost regions on the Qinghai-Tibet Plateau. It can be seen through our observation that the different freeze-thaw stages of active layer strongly regulated the  $R_s$  emissions and the  $R_s$  emission models and  $SR$  (sum soil respiration) among the different freeze-thaw stages were significantly different. The mean  $R_s$  flux ( $1.75\pm 0.37\mu\text{mol}/\text{m}^2\text{s}$ ) in the ST stage was 1.20, 1.97, and 3.11 times higher than those in the AF ( $1.46\pm 0.39$ ), WC ( $0.89\pm 0.42$ ), and SW ( $0.56\pm 0.10$ ) stages, respectively. Due to the longer duration (157 days) and higher  $R_s$  flux,  $SR$  in the ST stage was approximately estimated to be 60% of annual soil respiration; and the total  $SR$  in the AF, WC and SW stages accounted for 40% of annual emissions, being consistent with results for another alpine meadow region on the QTP during non-growing seasons (Zhang et al., 2015a). The higher annual contribution of ST stage to the cumulative  $R_s$  is likely due to the unique seasonal climate of the plateau. More specifically, the Tibetan alpine meadow receives more than 60–90% precipitation in the ST stage, but maximum 10% in the other stages (Xu et al., 2008). In addition, higher soil temperature and sufficient soil water content in the wet and humid summers stimulated microbial activity and caused higher metabolic rates of soil organisms and roots (Keith et al., 1997). In the alpine ecosystem regions underlain by permafrost on the Qinghai-Tibet Plateau, ten consecutive years of observation has found that the near-surface permafrost is warming, causing the active layer thickness to increase at  $4.26\text{cm}/\text{a}$  and the duration of thawing to increase by at least 14 days (Wu et al., 2015), which would emit significantly more  $R_s$  in the ST stage. Although



the AF, WC, and SW stages were in the frozen period, and the durations were short for AF (28 days),  
295 WC (92 days), and SW (89 days) stages, the cumulative  $R_s$  in these three stages contributed  
significantly to annual  $R_s$ . This may be attributed to the high-temperature sensitivities of soil  
respiration and the maintenance of soil microbial activities at extremely low temperatures (Panikov  
et al., 2006), resulting in the high rate of soil organic carbon decomposition (Monson et al., 2006).

Meanwhile, the development of freezing and thawing process also modified the temperature  
300 sensitivity of soil respiration ( $Q_{10}$ ) due to seasonal variations in temperature, water, plant phenology  
and substrate availability (Jiang et al., 2018; Contosta et al., 2013). In the current study, we found  
large variations in  $Q_{10}$  among the different freeze-thaw stages, with the maximum (4.9) in the WC  
stage and minimum (1.7) in the SW stage. The  $Q_{10}$  value (2.2) in the ST stage was smaller than that  
in the WC stage but higher than that in the SW stage. It has been previously reported that the  $Q_{10}$   
305 values in the frozen period are high. For example, in the freezing dormant season of a semiarid  
ecosystem in the Loess Plateau of China, the mean  $Q_{10}$  value reached 4.0 relative to 1.0 in the warm  
season (Shi et al., 2012); and the  $Q_{10}$  was 10.5 during the freezing process in the boreal forests (Du  
et al., 2013). In the warm season, the  $R_s$  mainly originated from auto- and heterotrophic components,  
but in cold season  $R_s$  was mostly composed by the heterotrophic component. Therefore, this seasonal  
310 variation in the composition of the soil microbial community may lead to higher  $Q_{10}$  in the frozen  
period. It was found that microbes living in summer cannot survive in winter below 4°C (Monson et  
al., 2006), and those who have adapted to freezing conditions grew exponentially with increasing  
temperature. Furthermore, the soil freezing decreased in liquid water and might invoke a physical  
limitation to substrate diffusion and render  $R_s$  more sensitive to temperature (Schimel and Mikan,  
315 2005). So when the freeze-thaw process shifted from ST stage to AF stage, and to the WC stage, the  
 $Q_{10}$  value increased. When it came to the SW stage, due to the soil still being kept frozen and the  
labile substrate being consumed in the previous stages, the activation energy supply was low (Wang  
et al., 2014) and the decomposition of recalcitrant substrates was limited, resulting in a sharp  
decrease of  $Q_{10}$ . Whatever the underlying mechanism, the high performance ( $R^2=0.55-0.90$ ) of the  
320  $R_s$  model in the different freeze-thaw stages, along with the high  $Q_{10}$  indicated that the potential  
magnitude of  $R_s$  may be increased with global warming.

#### 4.2 Effects of soil temperature and soil water content in each freeze-thaw stage on

##### $R_s$

$R_s$  values were sensitive to soil temperature changes during the different freeze-thaw stages.  
325 When the soil water content was sufficient,  $R_s$  was mainly dependent on the soil temperature. In the  
present study, we observed that the striking results in Figure 4 showed a significant increase in  $R_s$   
with a CO<sub>2</sub> emission peak in August as the soil warmed and soil water content arose in the first half  
of the ST stage. When it came to the latter half of the ST stage, although the soil water content at  
5cm decreased dramatically, the  $R_s$  still emitted at a high rate and declined with fluctuations with  
330 soil temperature. This phenomenon may have been caused by an acceleration of microbial activity  
because the soil temperature increased, and sufficient soil water content made the organic substrates  
release largely (Kurganova et al., 2007). In addition, soil water content was not a determinative  
factor affecting soil respiration under the condition that it was adequate.

When it came to the AF stage, although the surface soil temperature declined sharply and the  
335 freezing process began to develop upwards from the bottom of the active layer, the  $R_s$  flux was still  
kept at a relatively stable rate (1.20 μmol/m<sup>2</sup>s) in the UF substage because the soil water content was



still enough ( $SWC > 14\%$ ) and the surface soil was still in a thawed state. While at the transition time between UF substage and ZC substage, the  $R_s$  flux decreased suddenly to a minimum ( $1.14 \mu\text{mol}/\text{m}^2\text{s}$ ), and then increased sharply to a maximum ( $2.09 \mu\text{mol}/\text{m}^2\text{s}$ ); it fell again with fluctuation. The mechanism for the dramatical change in  $R_s$  efflux in this AF stage is not absolutely clear. One possible explanation is that microbes are warm-adapted and more sensitive to  $T_s$  when the freezing process is initiated. Furthermore, the process of the diurnal freezing-thawing cycle of surface soil also happened in the earlier ZC substage, and  $R_s$  increased rapidly from a very low level over diurnal cycle, indicating that microbes responded rapidly to minor changes in  $T_s$  even within several hours (Liu et al., 2016). As the freezing process developed rapidly downwards from the surface soil and upwards from the bottom of the active layer in the ZC substage, the trapped  $\text{CO}_2$  in the soil pores would be squeezed out and released during the transition of soil moisture from the liquid to solid state, leading to a dramatically fluctuating  $R_s$ .

In the WC stage, we observed that the  $R_s$  decreased synchronously as the soil temperature and water content continued to decline, but the  $R_s$  rate never reached zero although the soil of active layer was frozen completely, indicating that the soil microorganisms could maintain their activities at extremely low temperatures (Panikov et al., 2006). This result well agreed with other laboratory researches (Kurganova et al., 2007; Panikov and Dedysh, 2000). The continued decrease in soil temperature and liquid water content resulted in a partial death of microbes (Walker et al., 2006), and the microbial activities and substrate affinity were reduced (Nedwell, 1999), causing a continuous decline in the  $R_s$  flux. However, not all cells in the soil were killed or irreversibly damaged by the sustained low temperature and the dropping in soil water content (Walker et al., 2006), and the cold-adapted microflora still breathed and consumed the limited liberated nutrients in the frozen soil (Kurganova et al., 2007). Consequently, the  $R_s$  flux always maintained a level higher than zero.

In the SW stage, we found that although the active layer still remained frozen, the  $R_s$  flux and the surface soil temperature ( $T_s$ ) began to synchronously increase with fluctuation; the soil water content ( $SWC$ ) changed very little (around  $0.06 \text{ m}^3\text{m}^{-3}$ ) during the previous stage but varied with great fluctuation during the latter stage because the surface soil underwent spring diurnal freeze-thaw process. This phenomenon indicated that the soil temperature ( $T_s$ ) was the most important driver of  $R_s$  in this stage, and the cold-adapted microbes became much more sensitive to increase in  $T_s$  (Tribelli and López, 2018; Razavi et al., 2017), causing the  $R_s$  to increase rapidly from a low level. In addition, during the spring diurnal freeze-thaw process in the latter SW stage, the surface soil temperature dropped quickly to  $< 0^\circ\text{C}$  in the night and solar radiation again warmed the surface soil and induced the surface soil to thaw in the day (Wang et al., 2016; Bristow and Campbell, 1984). Therefore the  $SWC$  changed with great fluctuation, and the  $R_s$  was enhanced and its emission rate was maintained at a high level with fluctuation due to the soil microbes being activated by repeatedly freezing and thawing actions.

## 5 Conclusions

The freezing and thawing process of active layer significantly regulated the soil respiration of the alpine meadow in permafrost region on the Qinghai-Tibet Plateau. The soil temperature was the key factor affecting soil respiration regardless of soil water status during each freeze-thaw stage. The cumulated soil respiration in different freeze-thaw stages ranged from 60.57 to 1041.85  $\text{gCO}_2\text{m}^{-2}$ , and the cumulated soil respiration in the ST, AF, WC, and SW stages contributed 61.54, 8.89,



380 18.35, and 11.22% of annual  $R_s$  emissions, respectively. At the transition time of diurnal freeze-thaw  
cycle, we found that the dramatical variations in  $R_s$  in the AF stage may be caused by the inactivated  
warm-adapted microbes due to rapid dropping in temperature and the extruded  $\text{CO}_2$  from soil pores  
due to freezing, and the vigorous variations in  $R_s$  in the SW stage may be attributed to the cold-  
385 adapted microbes being activated by repeatedly freezing and thawing actions and becoming much  
more sensitive to increase in temperature. Furthermore, in the scenario of future climate projections  
of warmer temperature, great changes in freeze-thaw process patterns may have an important  
impacts on  $R_s$ . Further research is required to define the regulatory mechanism and its key processes  
on  $R_s$  in different freeze-thaw stages of the active layer.

### Acknowledgments

390 This study was supported by the National Natural Science Foundation of China (41771080,  
41701066, 41003032), the Fund of State Key Laboratory of Frozen Soil Engineering (No. SKLFSE-  
ZT-36) and the grant of China Scholarship Council. We are grateful to Dr. Yali Liu and Yu Gao for  
their help in the field measurement of soil  $\text{CO}_2$  flux. We gratefully thank the reviewers for their  
comments.

### 395 References

- Bond-Lamberty, B., and Thomson, A.: Temperature-associated increases in the global soil respiration  
record, *Nature*, 464, 579, 2010.
- Bristow, K. L., and Campbell, G. S.: On the relationship between incoming solar radiation and daily  
maximum and minimum temperature, *Agricultural and forest meteorology*, 31, 159-166, 1984.
- 400 Celis, G., Mauritz, M., Bracho, R., Salmon, V. G., Webb, E. E., Hutchings, J., Natali, S. M., Schädel, C.,  
Crummer, K. G., and Schuur, E. A. G.: Tundra is a consistent source of  $\text{CO}_2$  at a site with progressive  
permafrost thaw during 6 years of chamber and eddy covariance measurements, *Journal of Geophysical  
Research: Biogeosciences*, 122, 1471-1485, 10.1002/2016jg003671, 2017.
- Chen, X., Wang, G., Zhang, T., Mao, T., Wei, D., Hu, Z., and Song, C.: Effects of warming and nitrogen  
405 fertilization on GHG flux in the permafrost region of an alpine meadow, *Atmospheric environment*, 157,  
111-124, 2017.
- Commene, R., Lindaas, J., Benmergui, J., Luus, K. A., Chang, R. Y. W., Daube, B. C., Euskirchen, E. S.,  
Henderson, J. M., Karion, A., Miller, J. B., Miller, S. M., Parazoo, N. C., Randerson, J. T., Sweeney, C.,  
Tans, P., Thoning, K., Veraverbeke, S., Miller, C. E., and Wofsy, S. C.: Carbon dioxide sources from  
410 Alaska driven by increasing early winter respiration from Arctic tundra, *Proceedings of the National  
Academy of Sciences*, 114, 5361, 10.1073/pnas.1618567114, 2017.
- Contosta, A. R., Frey, S. D., Ollinger, S. V., and Cooper, A. B.: Soil respiration does not acclimatize to  
warmer temperatures when modeled over seasonal timescales, *Biogeochemistry*, 112, 555-570, 2013.
- Davidson, E. A., Belk, E., and Boone, R. D.: Soil water content and temperature as independent or  
415 confounded factors controlling soil respiration in a temperate mixed hardwood forest, *Global change  
biology*, 4, 217-227, 1998.
- Davidson, E. A., and Janssens, I. A.: Temperature sensitivity of soil carbon decomposition and feedbacks  
to climate change, *Nature*, 440, 165, 2006.
- Ding, J., Zhang, Y., Wang, M., Sun, X., Cong, J., Deng, Y., Lu, H., Yuan, T., Van Nostrand, J. D., and Li,  
420 D.: Soil organic matter quantity and quality shape microbial community compositions of subtropical  
broadleaved forests, *Molecular ecology*, 24, 5175-5185, 2015.



- Du, E., Zhou, Z., Li, P., Jiang, L., Hu, X., and Fang, J.: Winter soil respiration during soil-freezing process in a boreal forest in Northeast China, *Journal of Plant Ecology*, 6, 349-357, 2013.
- Grogan, P., and Chapin Iii, F.: Initial effects of experimental warming on above-and belowground components of net ecosystem CO<sub>2</sub> exchange in arctic tundra, *Oecologia*, 125, 512-520, 2000.
- 425 Henry, H. A.: Soil freeze–thaw cycle experiments: trends, methodological weaknesses and suggested improvements, *Soil Biology and Biochemistry*, 39, 977-986, 2007.
- Hollesen, J., Elberling, B., and Jansson, P.-E.: Future active layer dynamics and carbon dioxide production from thawing permafrost layers in Northeast Greenland, *Global Change Biology*, 17, 911-926, 2011.
- 430 Janssens, I. A., and Pilegaard, K.: Large seasonal changes in Q<sub>10</sub> of soil respiration in a beech forest, *Global Change Biology*, 9, 911-918, 2003.
- Jiang, H., Zhang, W., Yi, Y., Yang, K., Li, G., and Wang, G.: The impacts of soil freeze/thaw dynamics on soil water transfer and spring phenology in the Tibetan Plateau, Arctic, Antarctic, and Alpine Research, 50, e1439155, 2018.
- 435 Jiao, Y., and Li, R.: Processes of soil thawing-freezing and features of soil moisture migration in the permafrost active layer, *Journal of Glaciology and Geocryology*, 36, 237-247, 2014.
- Jobbágy, E. G., and Jackson, R. B.: The vertical distribution of soil organic carbon and its relation to climate and vegetation, *Ecological applications*, 10, 423-436, 2000.
- 440 Jorgenson, M., and Osterkamp, T. E.: Response of boreal ecosystems to varying modes of permafrost degradation, *Canadian Journal of Forest Research*, 35, 2100-2111, 2005.
- Keith, H., Jacobsen, K., and Raison, R.: Effects of soil phosphorus availability, temperature and moisture on soil respiration in *Eucalyptus pauciflora* forest, *Plant and Soil*, 190, 127-141, 1997.
- Knowles, J. F., Blanken, P. D., Lawrence, C. R., and Williams, M. W.: Evidence for non-steady-state carbon emissions from snow-scoured alpine tundra, *Nature Communications*, 10, 1306, 10.1038/s41467-019-09149-2, 2019.
- 445 Kurganova, I., Teepe, R., and Loftfield, N.: Influence of freeze-thaw events on carbon dioxide emission from soils at different moisture and land use, *Carbon balance and management*, 2, 2, 2007.
- Li, R., Zhao, L., Ding, Y., Wu, T., Xiao, Y., Du, E., Liu, G., and Qiao, Y.: Temporal and spatial variations of the active layer along the Qinghai-Tibet Highway in a permafrost region, *Chinese Science Bulletin*, 57, 4609-4616, 2012.
- Liu, B., Mou, C., Yan, G., Xu, L., Jiang, S., Xing, Y., Han, S., Yu, J., and Wang, Q.: Annual soil CO<sub>2</sub> efflux in a cold temperate forest in northeastern China: effects of winter snowpack and artificial nitrogen deposition, *Scientific reports*, 6, 18957, 2016.
- 455 Liu, X., and Chen, B.: Climatic warming in the Tibetan Plateau during recent decades, *International journal of climatology*, 20, 1729-1742, 2000.
- Lloyd, J., and Taylor, J.: On the temperature dependence of soil respiration, *Functional ecology*, 315-323, 1994.
- Lüers, J., Westermann, S., Piel, K., and Boike, J.: Annual CO<sub>2</sub> budget and seasonal CO<sub>2</sub> exchange signals at a high Arctic permafrost site on Spitsbergen, Svalbard archipelago, *Biogeosciences*, 11, 6307-6322, 10.5194/bg-11-6307-2014, 2014.
- 460 MacDougall, A. H., Avis, C. A., and Weaver, A. J.: Significant contribution to climate warming from the permafrost carbon feedback, *Nature Geoscience*, 5, 719, 2012.
- Monson, R. K., Lipson, D. L., Burns, S. P., Turnipseed, A. A., Delany, A. C., Williams, M. W., and Schmidt, S. K.: Winter forest soil respiration controlled by climate and microbial community
- 465



- composition, *Nature*, 439, 711, 2006.
- Mu, C., Zhang, T., Wu, Q., Peng, X., Cao, B., Zhang, X., and Cheng, G.: Organic carbon pools in permafrost regions on the Qinghai–Xizang (Tibetan) Plateau, *The Cryosphere*, 9, 479-486, 2015.
- 470 Nedwell, D. B.: Effect of low temperature on microbial growth: lowered affinity for substrates limits growth at low temperature, *FEMS microbiology ecology*, 30, 101-111, 1999.
- Panikov, N., Flanagan, P., Oechel, W., Mastepanov, M., and Christensen, T.: Microbial activity in soils frozen to below– 39 C, *Soil Biology and Biochemistry*, 38, 785-794, 2006.
- Panikov, N. S., and Dedysh, S.: Cold season CH<sub>4</sub> and CO<sub>2</sub> emission from boreal peat bogs (West Siberia): Winter fluxes and thaw activation dynamics, *Global Biogeochemical Cycles*, 14, 1071-1080, 2000.
- 475 Phillips, C. L., Nickerson, N., Risk, D., and Bond, B. J.: Interpreting diel hysteresis between soil respiration and temperature, *Global Change Biology*, 17, 515-527, 2011.
- Ping, C.-L., Michaelson, G. J., Jorgenson, M. T., Kimble, J. M., Epstein, H., Romanovsky, V. E., and Walker, D. A.: High stocks of soil organic carbon in the North American Arctic region, *Nature Geoscience*, 1, 615, 2008.
- 480 Razavi, B. S., Liu, S., and Kuzyakov, Y.: Hot experience for cold-adapted microorganisms: temperature sensitivity of soil enzymes, *Soil Biology and Biochemistry*, 105, 236-243, 2017.
- Schimel, J. P., and Mikan, C.: Changing microbial substrate use in Arctic tundra soils through a freeze-thaw cycle, *Soil Biology and Biochemistry*, 37, 1411-1418, 2005.
- Schlesinger, W. H., and Andrews, J. A.: Soil respiration and the global carbon cycle, *Biogeochemistry*, 48, 7-20, 2000.
- 485 Schneider von Deimling, T., Meinshausen, M., Levermann, A., Huber, V., Frieler, K., Lawrence, D., and Brovkin, V.: Estimating the near-surface permafrost-carbon feedback on global warming, *Biogeosciences*, 9, 649-665, 2012.
- Schuur, E. A., Bockheim, J., Canadell, J. G., Euskirchen, E., Field, C. B., Goryachkin, S. V., Hagemann, S., Kuhry, P., Laflour, P. M., and Lee, H.: Vulnerability of permafrost carbon to climate change: Implications for the global carbon cycle, *BioScience*, 58, 701-714, 2008.
- 490 Shi, W.-Y., Zhang, J.-G., Yan, M.-J., Yamanaka, N., and Du, S.: Seasonal and diurnal dynamics of soil respiration fluxes in two typical forests on the semiarid Loess Plateau of China: Temperature sensitivities of autotrophs and heterotrophs and analyses of integrated driving factors, *Soil Biology and Biochemistry*, 52, 99-107, 2012.
- 495 Tarnocai, C.: The impact of climate change on Canadian peatlands, *Canadian Water Resources Journal*, 34, 453-466, 2009.
- Tribelli, P., and López, N.: Reporting key features in cold-adapted bacteria, *Life*, 8, 8, 2018.
- 500 Walker, V. K., Palmer, G. R., and Voordouw, G.: Freeze-thaw tolerance and clues to the winter survival of a soil community, *Appl. Environ. Microbiol.*, 72, 1784-1792, 2006.
- Walz, J., Knoblauch, C., Böhme, L., and Pfeiffer, E.-M.: Regulation of soil organic matter decomposition in permafrost-affected Siberian tundra soils-Impact of oxygen availability, freezing and thawing, temperature, and labile organic matter, *Soil Biology and Biochemistry*, 110, 34-43, 2017.
- 505 Wang, J., and Wu, Q.: Impact of experimental warming on soil temperature and moisture of the shallow active layer of wet meadows on the Qinghai-Tibet Plateau, *Cold Regions Science and Technology*, 90, 1-8, 2013.
- Wang, K., Zhang, T., Guo, H., and Wang, H.: Climatology of the timing and duration of the near-surface soil freeze-thaw status across China, Arctic, Antarctic, and Alpine Research, 48, 723-738, 2016.
- Wang, Y., Liu, H., Chung, H., Yu, L., Mi, Z., Geng, Y., Jing, X., Wang, S., Zeng, H., and Cao, G.: Non -



- 510 growing - season soil respiration is controlled by freezing and thawing processes in the summer  
monsoon - dominated Tibetan alpine grassland, *Global Biogeochemical Cycles*, 28, 1081-1095, 2014.  
Webb, E., Schuur, E., Natali, S., Oken, K., Bracho, R., Krapek, J., Risk, D., and Nickerson, N.: Increased  
wintertime CO<sub>2</sub> loss as a result of sustained tundra warming, *Journal of Geophysical Research:*  
*Biogeosciences*, 121, 10.1002/2014JG002795, 2016.
- 515 Wu, Q., Zhang, T., and Liu, Y.: Permafrost temperatures and thickness on the Qinghai-Tibet Plateau,  
*Global and Planetary Change*, 72, 32-38, 2010.  
Wu, Q., Hou, Y., Yun, H., and Liu, Y.: Changes in active-layer thickness and near-surface permafrost  
between 2002 and 2012 in alpine ecosystems, Qinghai-Xizang (Tibet) Plateau, China, *Global and*  
*Planetary Change*, 124, 149-155, 2015.
- 520 Xu, Z., Gong, T., and Li, J.: Decadal trend of climate in the Tibetan Plateau—regional temperature and  
precipitation, *Hydrological Processes: An International Journal*, 22, 3056-3065, 2008.  
Yang, M.-x., Yao, T.-d., He, Y.-q., Zhang, X.-j., and Ma, Y.-m.: The water cycles between land surface  
and atmosphere in northern part of Tibetan Plateau, *Scientia Geographica Sinica/Dili Kexue*, 22, 29-33,  
2002.
- 525 Yin, G., Niu, F., Lin, Z., Luo, J., and Liu, M.: Effects of local factors and climate on permafrost conditions  
and distribution in Beiluhe basin, Qinghai-Tibet Plateau, China, *Science of the Total Environment*, 581,  
472-485, 2017.  
Zhang, T., Wang, G., Yang, Y., Mao, T., and Chen, X.: Non-growing season soil CO<sub>2</sub> flux and its  
contribution to annual soil CO<sub>2</sub> emissions in two typical grasslands in the permafrost region of the  
530 Qinghai-Tibet Plateau, *European Journal of Soil Biology*, 71, 45-52, 2015a.  
Zhang, T., Wang, G., Yang, Y., Mao, T., and Chen, X.: Grassland types and season-dependent response  
of ecosystem respiration to experimental warming in a permafrost region in the Tibetan Plateau,  
*Agricultural and Forest Meteorology*, 247, 271-279, 2017.  
Zhang, Y., Gao, Q., Dong, S., Liu, S., Wang, X., Su, X., Li, Y., Tang, L., Wu, X., and Zhao, H.: Effects  
535 of grazing and climate warming on plant diversity, productivity and living state in the alpine rangelands  
and cultivated grasslands of the Qinghai-Tibetan Plateau, *The Rangeland Journal*, 37, 57-65, 2015b.  
Zhao, L., Cheng, G., Li, S., Zhao, X., and Wang, S.: Thawing and freezing processes of active layer in  
Wudaoliang region of Tibetan Plateau, *Chinese Science Bulletin*, 45, 2181-2187, 2000.  
Zimov, N., Zimov, S., Zimova, A., Zimova, G., Chuprynin, V., and Chapin III, F.: Carbon storage in  
540 permafrost and soils of the mammoth tundra - steppe biome: Role in the global carbon budget,  
*Geophysical Research Letters*, 36, 2009.



### Figure captions

Figure 1. Soil temperature contour outlines of the experimental site in 2017 and 2018

Figure 2. Variations of  $R_s$  flux at different freeze-thaw stages in years of 2017 and 2018. Error bars show standard error ( $n=6$ )

5 Figure 3. Sum of  $R_s$  ( $SR$ ) and its contribution for the four freeze-thaw stages including summer thawing stage (ST), autumn freezing stage (AF), winter cooling stage (WC) and spring warming stage (SW). The value above the bar is the percentage contribution of each freeze-thaw stage to annual total  $R_s$ .

10 Figure 4. Variations in soil respiration ( $R_s$ ), soil temperature ( $T_s$ ) and soil water content (SWC) for the four freeze-thaw stages including summer thawing stage (ST), autumn freezing stage (AF), winter cooling stage (WC), and spring warming stage (SW) (from later April 2017 to late April 2018). The SWC unit stands for water volume per total soil volume.

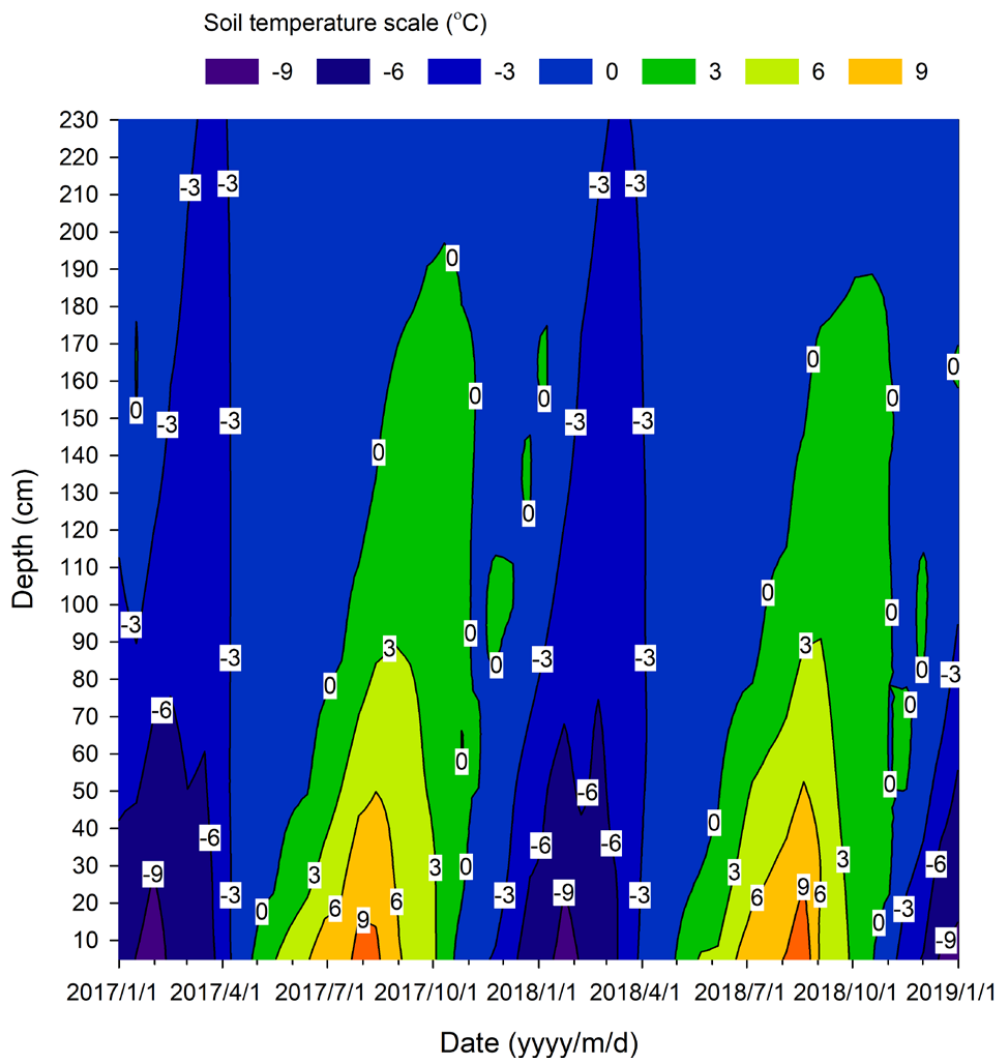


Figure 1

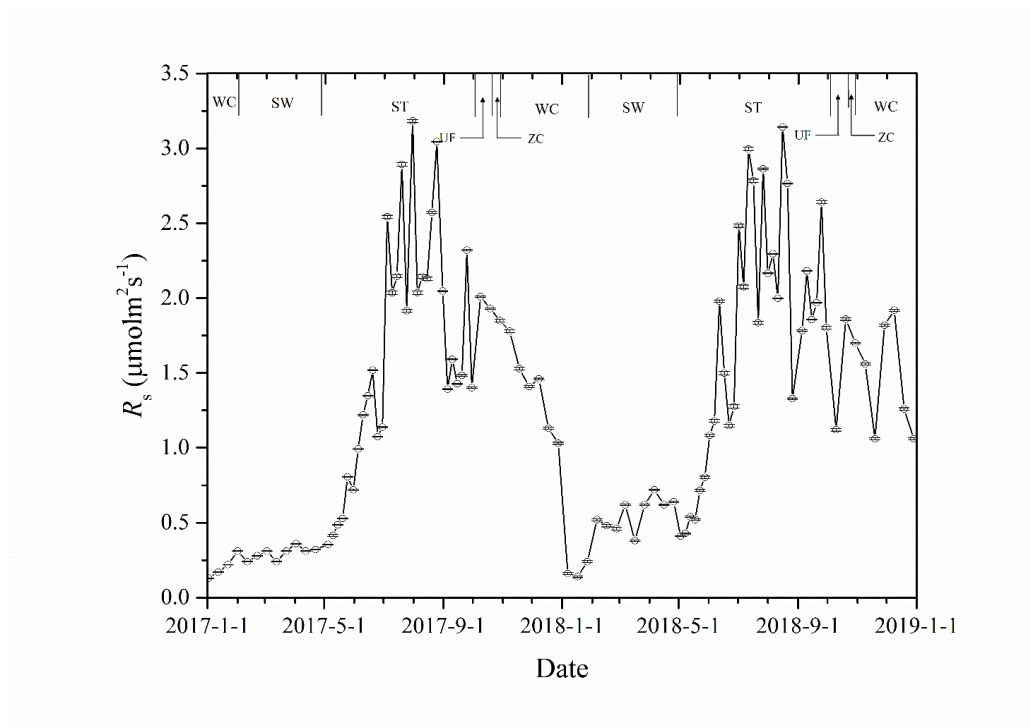


Figure 2

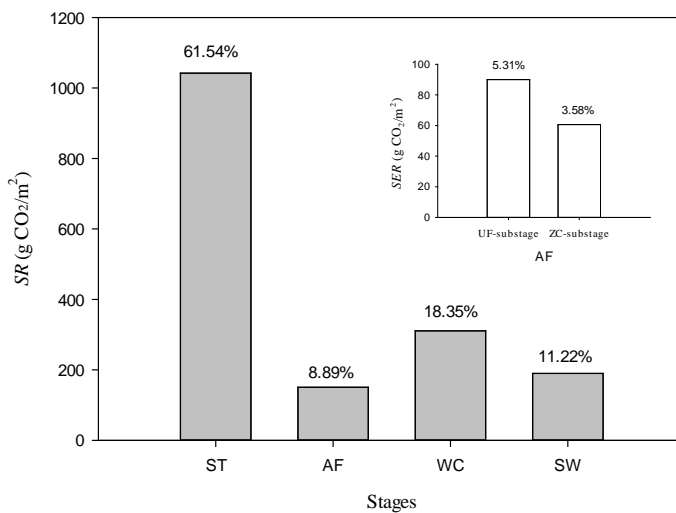


Figure 3

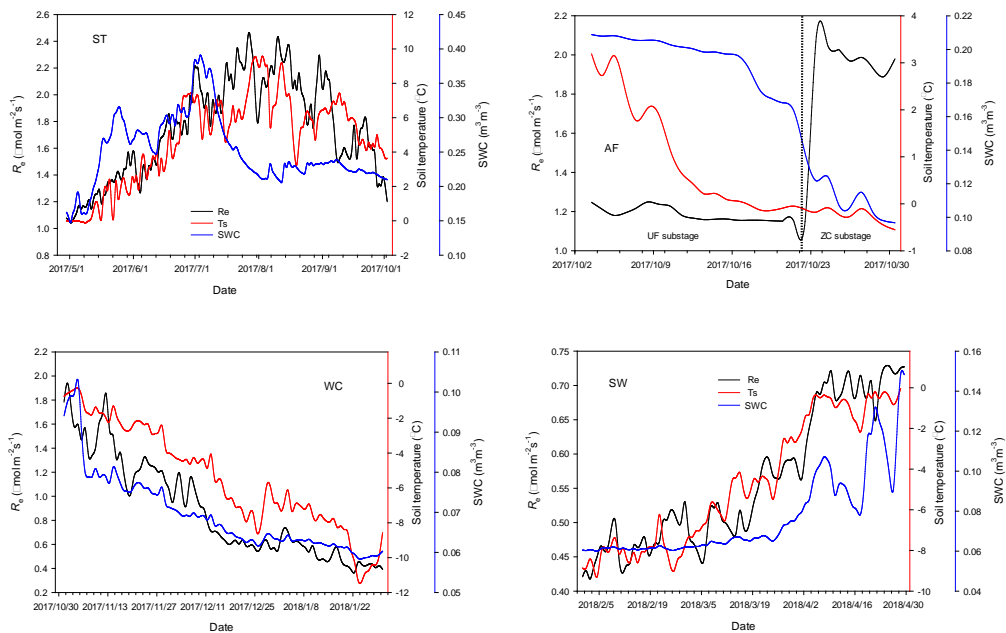


Figure 4